Atmos. Meas. Tech., 11, 2553–2565, 2018
https://doi.org/10.5194/amt-11-2553-2018

Atmospheric Measurement Techniques
Open Access
EGU

Detection of carbon monoxide pollution from cities and wildfires on regional and urban scales: the benefit of CO column retrievals from SCIAMACHY 2.3 µm measurements under cloudy conditions

Tobias Borsdorff, Josip Andrasec, Joost aan de Brugh, Haili Hu, Ilse Aben, and Jochen Landgraf

SRON Netherlands Institute for Space Research, Utrecht, the Netherlands

Correspondence: Tobias Borsdorff (t.borsdorff@sron.nl)

Received: 24 November 2017 – Discussion started: 5 December 2017
Revised: 6 April 2018 – Accepted: 18 April 2018 – Published: 3 May 2018

Abstract. In the perspective of the upcoming TROPOMI Sentinel-5 Precursor carbon monoxide data product, we discuss the benefit of using CO total column retrievals from cloud-contaminated SCIAMACHY 2.3 µm shortwave infrared spectra to detect atmospheric CO enhancements on regional and urban scales due to emissions from cities and wildfires. The study uses the operational Sentinel-5 Precursor algorithm SICOR, which infers the vertically integrated CO column together with effective cloud parameters. We investigate its capability to detect localized CO enhancements distinguishing between clear-sky observations and observations with low (< 1.5 km) and medium–high clouds (1.5–5 km). As an example, we analyse CO enhancements over the cities Paris, Los Angeles and Tehran as well as the wildfire events in Mexico–Guatemala 2005 and Alaska–Canada 2004. The CO average of the SCIAMACHY full-mission data set of clear-sky observations can detect weak CO enhancements of less than 10 ppb due to air pollution in these cities. For low-cloud conditions, the CO data product performs similarly well. For medium–high clouds, the observations show a reduced CO signal both over Tehran and Los Angeles, while for Paris no significant CO enhancement can be detected. This indicates that information about the vertical distribution of CO can be obtained from the SCIAMACHY measurements. Moreover, for the Mexico–Guatemala fires, the low-cloud CO data captures a strong outflow of CO over the Gulf of Mexico and the Pacific Ocean and so provides complementary information to clear-sky retrievals, which can only be obtained over land. For both burning events, enhanced CO values are even detectable with medium–high-cloud retrievals, confirming a distinct vertical extension of the pollution. The larger number of additional measurements, and hence the better spatial coverage, significantly improve the detection of wildfire pollution using both the clear-sky and cloudy CO retrievals. Due to the improved instrument performance of the TROPOMI instrument with respect to its precursor SCIAMACHY, the upcoming Sentinel-5 Precursor CO data product will allow improved detection of CO emissions and their vertical extension over cities and fires, making new research applications possible.

1 Introduction

Carbon monoxide (CO) is an atmospheric trace gas emitted mainly by incomplete combustion processes. Its oxidation with the hydroxyl radial (OH) represents its major sink (Spivakovsky et al., 2000). Because of its moderately long lifetime and its low background concentration (Holloway et al., 2000), it is an important tracer for atmospheric transport of pollution (Logan et al., 1981). From space, CO is measured by different satellite instruments with global coverage, e.g. MOPITT (Measurements of Pollution in the Troposphere; Deeter, 2003), AIRS (Atmospheric Infrared Sounder; McMillan, 2005), TES (Tropospheric Emission Spectrometer; Rinsland et al., 2006), IASI (Infrared Atmospheric Sounding Interferometer; Turquety et al., 2004) and SCIAMACHY (SCanning Imaging Absorption Spectrometer for Atmospheric CHartographY; Gloudemans et al., 2009; Frankenberg et al., 2005; Buchwitz et al., 2007; Gimeno García et al., 2011).

The presence of clouds may represent a challenge for remote sensing of CO from space. Here, light scattering, and

hence the shielding of the atmosphere below the cloud, affects the vertical sensitivity of the measurement. This hampers the retrieval of the vertically integrated total column of CO from cloudy observations, and different approaches have been proposed to cope with this problem. Deeter (2003), Buchwitz et al. (2004), de Laat et al. (2006) and Borsdorff et al. (2016) suggest that only observations under clear-sky conditions or weakly cloud contaminated conditions should be considered, assuming that the sensitivity to CO in the lower troposphere is sufficient to estimate the total CO column. A different approach is followed by Buchwitz et al. (2007), Gloudemans et al. (2009) and de Laat et al. (2012), who used vertical profiles of CH_4 and CO taken from model simulations to compensate for the reduced sensitivity when retrieving trace gas columns from cloud-contaminated measurements. In contrast, Rinsland et al. (2006), Borsdorff et al. (2017) and Vidot et al. (2012) discussed the retrieval of the CO column jointly with effective cloud parameters, resulting in a retrieved CO column with its vertical sensitivity, which reflects the effect of clouds on the light path and so includes the shielding effect of clouds. This approach is not limited to particular conditions of cloud coverage and so generalizes the above-mentioned techniques, providing a higher data yield.

The usefulness of CO total column from satellite observations have been demonstrated by several studies. For example, after temporal averaging of several years of IASI and SCIAMACHY CO measurements, Pommier et al. (2013), Buchwitz et al. (2007) and Clerbaux et al. (2008) detected the relatively weak CO enhancement of urban pollution in cities. Also, the pronounced enhancement of CO due to wildfires has been reported (e.g. Gloudemans et al., 2006; Buchwitz et al., 2007). Depending on the study, only clear-sky observations or both clear-sky and cloudy observations are used. Due to the different vertical sensitivity of the observations, the use of the data has to be considered with care. For moderately high clouds, observations might not be suited to detecting enhanced CO concentrations in the lower atmosphere because of the shielding of the atmosphere below the cloud. On the other hand, cloudy and clear-sky observations with different vertical CO sensitivities provide information on the vertical distribution of CO (Liu et al., 2014). Here, it is necessary to observe similar CO vertical distributions with different cloudiness, which will be met more frequently by upcoming CO missions with enhanced spatial sampling and resolution in combination with improved the data quality of the individual CO soundings. On 13 October 2017 the TROPOspheric Monitoring Instrument (TROPOMI) was successfully launched on the Sentinel-5 Precursor mission (S-5P). The mission objectives and requirements are provided by Veefkind et al. (2012).

It measures the Earth's reflected radiances in the ultraviolet, visible, near infrared and shortwave infrared spectral range with a spatial resolution of about $7 \times 7\,\mathrm{km}^2$ at subsatellite point and daily global coverage. Here, shortwave infrared (SWIR) observations in the 2.3 µm spectral region provide information on the CO total column amount. In recent years, the SWIR CO retrieval algorithm SICOR has been developed for the operational processing of TROPOMI data (Vidot et al., 2012; Landgraf et al., 2016b, a). TROPOMI's high signal-to-noise ratio (SNR) performance in the SWIR will provide clear-sky CO total column densities with vertical sensitivity throughout the atmosphere (e.g. Buchwitz et al., 2004; Gloudemans et al., 2008; Borsdorff et al., 2014) and with a precision $< 10\,\%$ for single clear-sky soundings (Landgraf et al., 2016b). However, even with the high spatial resolution and sampling of TROPOMI, a major part of the measurements is cloud contaminated (Krijger et al., 2005, 2011). To optimally explore the SWIR measurements, SICOR also retrieves CO for cloudy conditions over land and ocean, inferring effective cloud parameters (cloud optical thickness τ_{cld}, cloud centre height z_{cld}) together with trace gas columns (Vidot et al., 2012; Landgraf et al., 2016b). The TROPOMI CO data product comprises the estimate of the CO column, its noise estimate, effective cloud parameters and the CO column averaging kernel, which provides the sensitivity of the retrieved column with respect to changes in the true vertical CO profile. For example, for cloudy atmospheres, the averaging kernel reflects the shielding of the atmosphere below the cloud with a reduced CO sensitivity, equivalent to small values of the averaging kernel. Furthermore, the effective cloud parameters provide useful information e.g. to classify measurements by the type of cloud contamination.

We have applied the SICOR algorithm to the full SCIAMACHY 2.3 µm data set. Here, SCIAMACHY covers the TROPOMI SWIR band with the same spectral resolution but with inferior radiometric performance, spatial resolution and global coverage (Bovensmann et al., 1999). The SCIAMACHY CO data set was validated with TCCON/NDACC measurements for clear-sky observations over land (Borsdorff et al., 2016) and with TCCON and MOSAIC/IAGOS airborne measurements (Borsdorff et al., 2017) for cloud-contaminated measurements over land and oceans. In general, those studies found a good agreement with the validation data sets considering the high noise error of the SCIAMACHY CO data set. For most sites the bias is $< 10\,\mathrm{ppb}$, but it can increase significantly at CO hotspots due to representation errors in the validation. In this study, we discuss the benefit of using CO retrievals from cloud-contaminated SCIAMACHY 2.3 µm measurements with their intrinsic vertical sensitivity for the detection of CO pollution from cities and wildfires. We separate CO retrievals into clear-sky, low ($< 1.5\,\mathrm{km}$) and medium–high (1.5–5 km) cloud conditions. As an example, we discuss CO pollution over Tehran, Paris and Los Angeles as well as the wildfires in Mexico–Guatemala 2005 (Herrera, 2016) and Alaska–Canada 2004.

The paper is structured as follows: in Sect. 2, we present the SCIAMACHY CO data set. Section 3 analyses the benefit of using the SCIAMACHY CO retrievals under cloudy

conditions to detect wildfires, and Sect. 4 focuses on the CO emission from cities. Section 5 draws some conclusions on the upcoming TROPOMI CO data set. The summary and conclusions are given in Sect. 6, and finally, the availability of the data is stated.

2 SCIAMACHY CO data set and retrievals

The SCIAMACHY instrument was operational on ESA's ENVISAT satellite from January 2003 to April 2012. We utilize the SWIR measurements of SCIAMACHY in nadir observation geometry with a spatial resolution of about $120 \times 30\,\mathrm{km}^2$, a swath of 960 and global coverage in under 3 days (Bovensmann et al., 1999). In this study, we analyse the SICOR CO total column densities retrieved from individual SCIAMACHY 2.3 µm spectra for the entire period of the mission from January 2003 to April 2012. The CO data product consists of the estimates of the total column concentrations of CO, H_2O and HDO (c_{CO}, c_{H_2O}, c_{HDO}), the corresponding retrieval noise (ϵ_{CO}, ϵ_{H_2O}, ϵ_{HDO}), averaging kernels, effective cloud parameters (cloud optical thickness τ_{cld} and cloud height z_{cld}) and the SWIR Lambertian surface albedo. Auxiliary parameters like signal-to-noise ratio SNR_{max} of the measurement and number of retrieval iterations (N_{iter}) are also provided. SICOR uses the profile-scaling approach, discussed in detail by Vidot et al. (2012), Borsdorff et al. (2014) and Landgraf et al. (2016b). Here, cloud optical depth and height are estimated using prior knowledge about CH_4, ECMWF surface pressure and the observed CH_4 absorption in the 2.3 µm spectral fit window (Landgraf et al., 2016a). The CH_4 data were taken from a TM5 model run (Williams et al., 2013, 2014) spanning the entire mission period of SCIAMACHY with global $3 \times 2^{\circ 2}$ horizontal resolution and 3 h sampling time. The algorithm can also be used for SCIAMACHY CO data processing because of the similarity of the TROPOMI and SCIAMACHY observations. The specific SCIAMACHY settings, e.g. the selection of the retrieval window, are discussed by Borsdorff et al. (2017). The spectral range for the retrieval from 2311 to 2338 nm was chosen to compensate for the detector pixel loss in the later years of the mission but also to include a strong CH_4 absorption line, which is beneficial for the retrieval of the effective cloud parameters. Due to an ice layer on the SWIR detectors and the radiometric degradation of the instrument, the processing of SCIAMACHY CO data requires a radiometric recalibration of the SWIR spectra as described by Borsdorff et al. (2016).

In this study, we filter the SCIAMACHY CO data based on the number of iterations N_{iter} and the estimate of the retrieval noise, which we compared with σ, the difference between the 50th and 68th percentiles of the retrieval results for the different data ensembles. The data filter reads

1. $N_{iter} < 15$
2. $\epsilon_{CO} < 4.5\,\sigma_{CO}$
3. $\epsilon_{H_2O} < 4.5\,\sigma_{H_2O}$
4. $\epsilon_{HDO} < 4.5\,\sigma_{HDO}$.

For the analysis of air pollution from cities, we add an additional filter considering the median CO column μ_{CO} of the CO data set of the different cities:

5. $\mu_{CO} - 4.5\,\sigma_{CO} \le c_{CO} < \mu_{CO} + 4.5\,\sigma_{CO}$.

This filter removes outliers of our data sets, which we attribute to erroneous retrievals possibly caused by the instrument degradation rather than an atmospheric signal, for the selected cities. It enables us to detect the relatively weak CO enhancement above the cities after averaging the data over the entire mission period. In this study we consider clear-sky and cloudy-sky retrievals with cloud heights smaller than 5 km, which are divided into three categories in Table 1.

An important element of the CO data product is the column averaging kernel A, which provides the sensitivity of the retrieved CO column to changes in the true vertical profile ρ_{true} of CO (Rodgers, 2000), namely

$$c_{ret} = A\rho_{true} + \epsilon_{CO}\,, \quad (1)$$

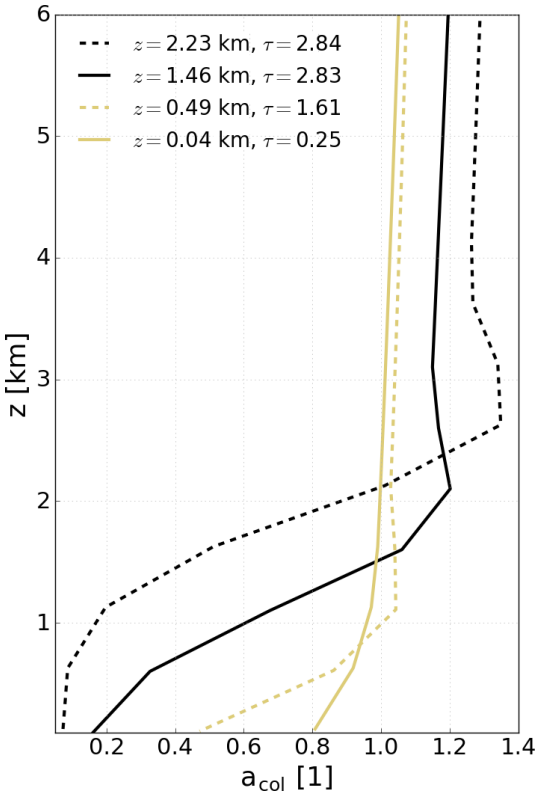

Figure 1. SCIAMACHY CO total column averaging kernels for different cloud centre heights (z_{cld}) and cloud optical thicknesses (τ_{cld}). Here, the solid yellow line is representative of clear-sky conditions. The figure shows typical cases of the vertical retrieval sensitivity of the SCIAMACHY CO retrievals over Paris.

Table 1. Categories of cloudy observations defined by the retrieved cloud optical depth τ_{cld}, the cloud height z_{cld} and the spectral maximum of the measurement SNR.

Category	Optical depth	Cloud height	SNR
Clear-sky observations	$\tau_{cld} < 2$	$z_{cld} < 0.5$ km	$SNR_{max} > 15$
Observations with low clouds	$\tau_{cld} > 2$	$z_{cld} < 1.5$ km	$SNR_{max} > 100$
Observations with medium–high cloud	$\tau_{cld} > 2$	1.5 km $< z_{cld} <$ 5 km	$SNR_{max} > 100$.

where ϵ_{CO} represents the error of the retrieved CO column caused by measurement errors. Equation (1) can be interpreted as a weighted altitude integration accounting for the vertical sensitivity of the retrieval to estimate the retrieved CO column density. Figure 1 shows the total column averaging kernels for four different cloud conditions over Paris. Here, scenes contaminated by optically thin low clouds provide a good vertical sensitivity of the total column of CO and so the values of A are close to 1 for all altitudes. However, for scenes with optically thick clouds, the retrieval loses CO sensitivity below the cloud with averaging kernel values well below 1. Because the CO column is estimated by a scaling of a reference profile, CO variations above a cloud also induce an adjustment of the CO concentration below the cloud, which the measurement is not sensitive to. This explains the column averaging kernel values > 1 at this altitude range (Borsdorff et al., 2016). This limited retrieval sensitivity to the atmospheric composition below cloud level induces the null-space error to the retrieved total column (e.g. Borsdorff et al., 2014). For the profile-scaling approach the magnitude of the null-space error depends, on the one hand, on the loss of vertical sensitivity and, on the other hand, on the discrepancy between the true vertical profile and the reference profile to be scaled by the inversion. Hence, depending on this discrepancy the retrieved column can over- or underestimate the true vertical column.

For individual CO retrievals from SCIAMACHY observations, the retrieval noise ϵ_{CO} can be high and can even exceed 100 % of the retrieved column depending on the SNR of the measurement (Gloudemans et al., 2008). Hence, for most applications individual SCIAMACHY CO retrievals need to be averaged to reduce the noise (de Laat et al., 2007; Gloudemans et al., 2006). In this study, we use an oversampling technique similar to the one used by Fioletov et al. (2011). This means that we first define an equidistant latitude–longitude grid with a sampling distance δ for a considered scene. For each grid cell, an averaged CO value is calculated using SCIAMACHY CO retrieval weighted with its noise error ϵ_{CO} within a circular domain of a radius r around the cell centre. Here $\delta < r$, which corresponds to an oversampling of the averaged SCIAMACHY CO field. To find an appropriate averaging radius r, a trade-off has to be made between the spatial resolution and the noise of the averaged CO field. Obviously, this choice depends on the particular application due the number of available CO data points and the brightness of the observed scene. The choice of the sampling distance δ is less critical for achieving an oversampling of the data field if it is $< r$. Therefore, r and δ changes for the applications discussed in the following are provided accordingly in the discussion. In the following, we chose r, such that a high spatial resolution is achieved but the retrieval noise is also sufficiently reduced by averaging. Hence, the choice of the parameter depends on the application, the number of individual retrievals available and the reflectivity of the ground scene. δ is less critical; however we chose it to be smaller than r to achieve an oversampling of the data.

3 CO pollution from wildfires

After carefully evaluating the SCIAMACHY CO data set, we selected two examples of wildfire events for further discussion: agricultural fires in Mexico–Guatemala 2005 and forest fires in Alaska–Canada 2004. Buchwitz et al. (2007) discussed the fires in Alaska–Canada 2004 with SCIAMACHY CO retrievals and Pfister et al. (2005) quantified their CO emissions using MOPITT CO data. We will revisit those fires from the perspective of CO retrievals under cloudy conditions.

Figure 2 shows time series of individual SCIAMACHY CO retrievals over Mexico for clear-sky, low-cloud and medium–high-cloud conditions as well as the daily GFED4 Burned Area product of MODIS (Randerson et al., 2017). Depending on the signal-to-noise ratio of the measurements, the retrieval noise of an individual CO retrieval can exceed 100 % of the retrieved column and through that can result in negative CO columns. It is important not to reject negative values when averaging data to avoid artificial biases (de Laat et al., 2007; Gloudemans et al., 2006).

The two burning events indicated by the GFED4 Burned Area product in 2003 and 2005 are clearly reflected in the time series of low-cloud and medium–high-cloud retrievals but shifted by about 45 days for both events. The reason for the shift is unclear and will be studied in future by looking at other satellite observations. As expected, CO retrieval values increase during the fire season (March–May) each year, coinciding with an increase in burned area. Here, the peak events are evident in both the low-cloud and medium–high-cloud data records. The time series of the clear-sky data is very noisy and has significant gaps because of the dark ocean surface in the SWIR which does not permit a CO retrieval. Both

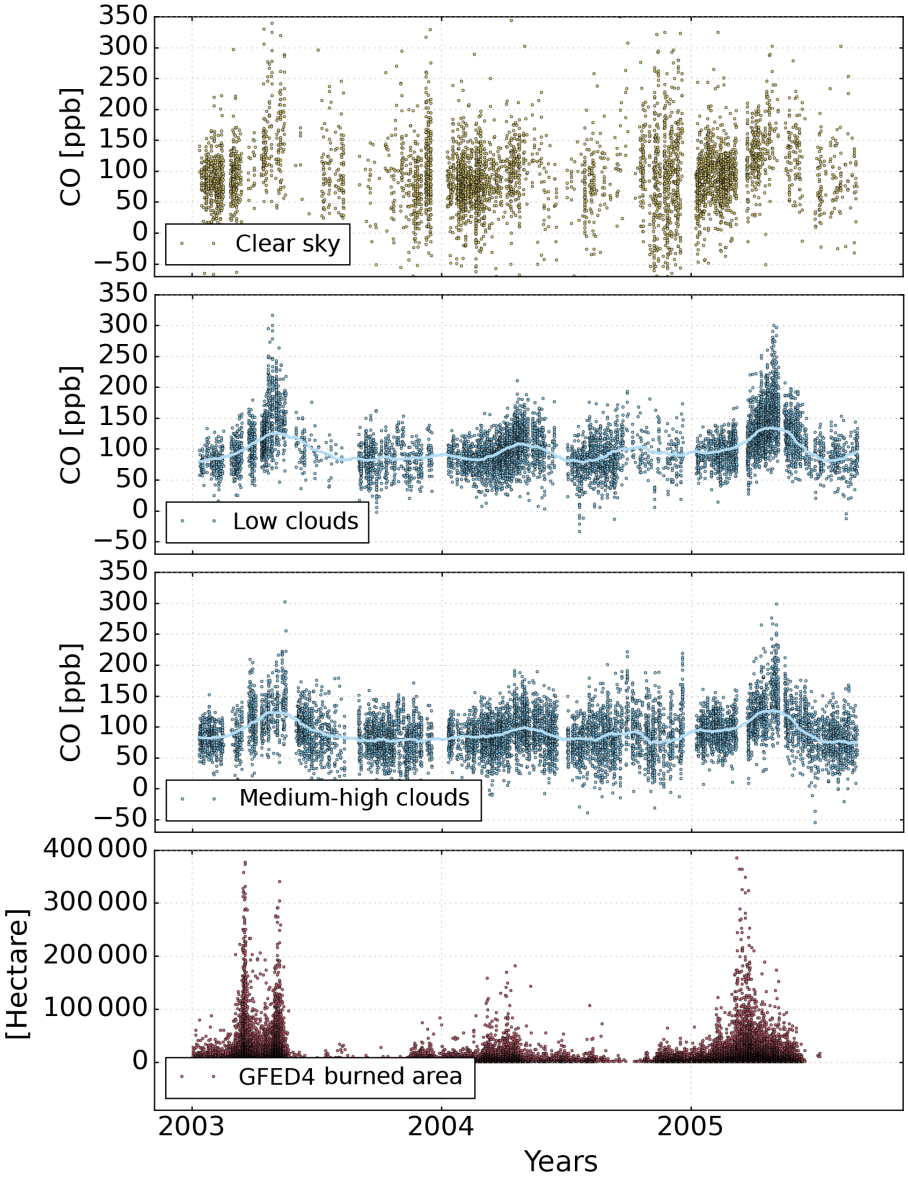

Figure 2. Individual SCIAMACHY CO retrievals under clear-sky, low cloud and medium–high-cloud atmospheric conditions as well as daily GFED4 Burned Area over Mexico–Guatemala in the latitude–longitude box (22.5° N, 100.0° W; 10.0° N, 80.0° W). The blue line is a running median with a half width of 30 days.

hamper the detection of fire events. Nonetheless, it seems that the two fire events are also visible in the clear-sky data.

From the clear-sky, low-cloud and medium–high-cloud time series we calculated daily mean values and investigated the correlation of the data sets. For the correlation between the low-cloud and clear-sky data product, the Pearson coefficient is 0.6 with a mean bias of 1.7 ppb and a standard deviation of the differences of 32.7 ppb. The large standard deviation reflects the noise in the clear-sky data. For the Mexico region, the land surface reflectivity, and so the corresponding SNR of the measurement is low, causing the high retrieval noise for clear-sky cases. However, the good correlation coefficient and the low bias shows that within the noise limitation the cloudy retrievals are in good agreement with the clear-sky retrievals.

The situation differs when inspecting the CO time series for SCIAMACHY observations with low- and medium–high-cloud coverage. Here the data are much less noisy. In the SWIR, clouds are highly reflective, as demonstrated by Borsdorff et al. (2017) using SCIAMACHY SWIR observations, and so the improved SNR of the SCIAMACHY measurements causes reduced noise in the CO data product. When correlating the low-cloud and the high-cloud retrievals, we find a Pearson correlation coefficient of 0.8, a

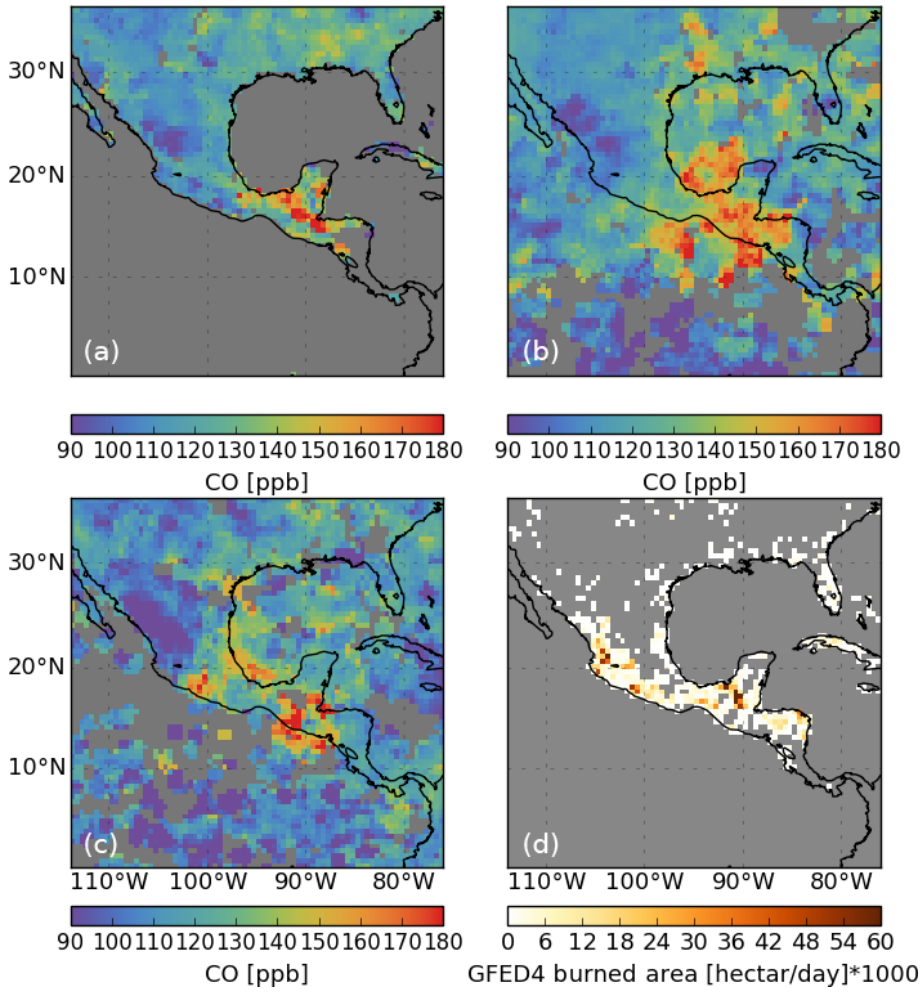

Figure 3. SCIAMACHY CO retrievals under clear-sky **(a)**, low-cloud **(b)** and medium–high cloud **(c)** atmospheric condition as well as daily GFED4 Burned Area **(d)** averaged from 15 March to 15 May 2005 over Mexico and Central America. The resolution of the plot is 0.5° in latitude and longitude and the data are oversampled using a radius of 90 km.

bias of 4.6 ppb and a standard deviation of the differences of 14 ppb. This supports our finding that both low-cloud and medium–high-cloud retrievals can capture the burning events equally well, something one may expect since CO pollution from wildfires constitutes a strong source that can reach the free troposphere (see Yurganov et al., 2005). If the CO plume was confined to the near-surface atmosphere, it would be more difficult if not impossible to sense it with cloudy observations. If the CO plume was confined near the surface it would be more difficult to sense it with cloudy retrievals.

Figure 3 shows the spatial distribution of the SCIAMACHY CO total column over Mexico for the period 15 March–15 May 2005 and the corresponding GFED4 Burned Area product. The SCIAMACHY data are averaged over an area with a radius $r = 90$ km and are subsequently oversampled with a longitude–latitude sampling distance of $\delta = 0.5°$ (≤ 55 km). We used the same latitude–longitude grid for the MODIS data and summed up the burned areas for the individual grid cells. Here, the clear-sky SCIAMACHY CO data clearly show the burning hotspot around the state Yucatán Peninsula in Mexico, also indicated by the MODIS Burned Area product. Some fires shown by the MODIS data are not reflected by the SCIAMACHY CO data, which may be explained by the fact that the CO emission of these fires is not sufficient to be detected with SCIAMACHY observations. For low-cloud conditions, the retrieval provides additional information showing the transport of air with high CO concentration into the Gulf of Mexico and over the Pacific Ocean, in agreement with the smoke detection of the MODIS Aqua instrument (https://earthobservatory.nasa.gov/NaturalHazards/view.php?id=14748, last access: 30 April 2018). Also, the earlier burning event in Mexico 2003 in Fig. 2 followed a similar transport pattern of enhanced CO over the oceans (as shown in Fig. 4). The CO observations with medium–high-cloud observations still reflect the CO enhancements but the

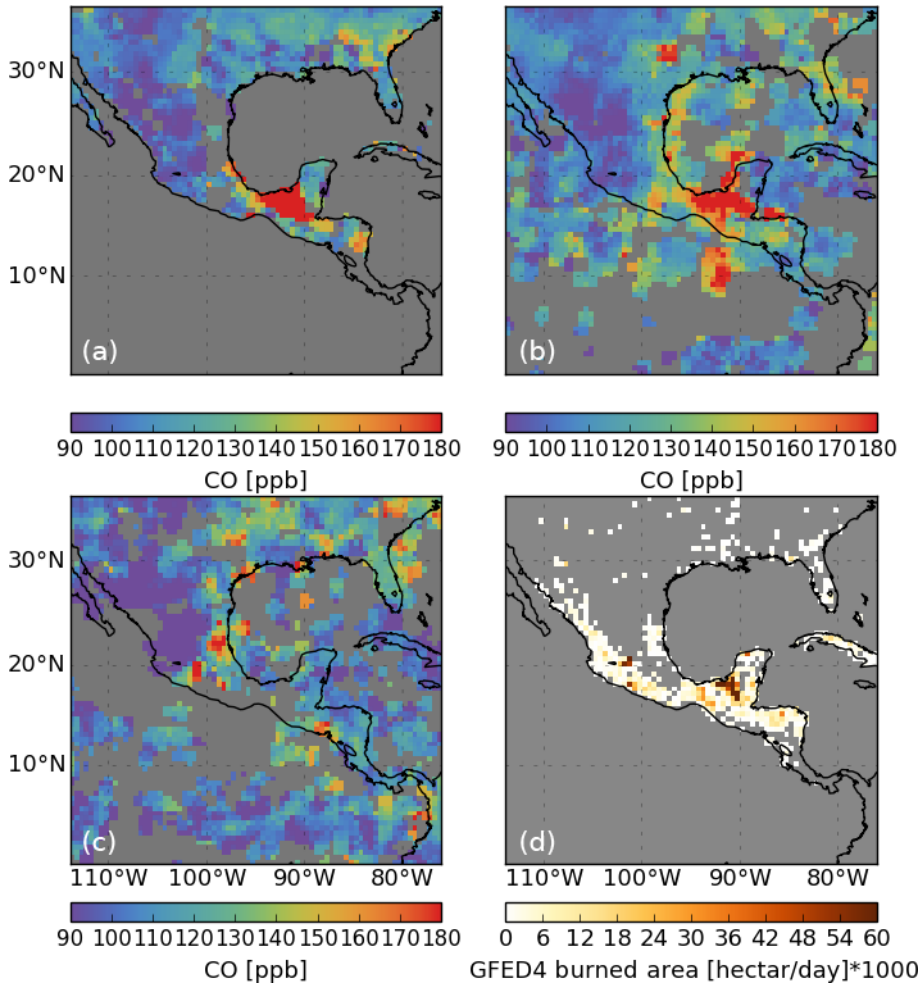

Figure 4. Same as Fig. 3, but the data are averaged from 1 April to 15 May 2003.

measurement density is too low to fully capture the event. Analogously, Fig. 5 shows the forest fires in Alaska–Canada from 1 July to 1 August 2004 using the same oversampled approach as in Fig. 3. Because of differences in meteorology, clear-sky observations are less frequent for the Alaska fires than for fires in Mexico, and hence clear-sky and low-cloud observations do not fully capture the Alaska 2004 fire event. For medium–high clouds, the corresponding CO product shows much better coverage and so can detect enhanced CO concentration transported away from the fires as indicated by the MODIS Burned Area product. In particular, this finding agrees with the study by Pfister et al. (2005), who reported enhanced CO concentration even high up in the atmosphere at about 400 hPa due to the Alaska fires.

The benefit of using cloudy observations to detect the transport of enhanced CO concentration from wildfires also becomes clear when comparing the number of individual SCIAMACHY CO sounding in Fig. 6. For the considered area of the Mexico fires, the 2402 individual clear sky soundings are more than doubled (6126 soundings) when we consider low-cloud observations, partly due to additional soundings over ocean which cannot be exploited for clear-sky conditions. Additionally 3225 soundings are found with medium–high clouds. For the Alaska fires, the relative distribution changes according to the meteorological situation but confirms a significant gain in the number of observations when including cloudy measurements. Here, we obtain 1473 clear-sky soundings, 2454 low-cloud soundings and 4819 medium–high-cloud soundings. Due to this, the means with which to observe enhanced CO values by pollution transport from wildfires with SCIAMACHY is clearly improved by using cloudy observations in addition to clear-sky observations.

4 CO pollution from cities

In this section, we selected the three cities Paris, Tehran and Los Angeles to discuss the relevance of cloudy observations for the detection of urban pollution. We accumulated all SCIAMACHY observations from 2003 to April 2012 around these cities, distinguishing between clear-sky, low-

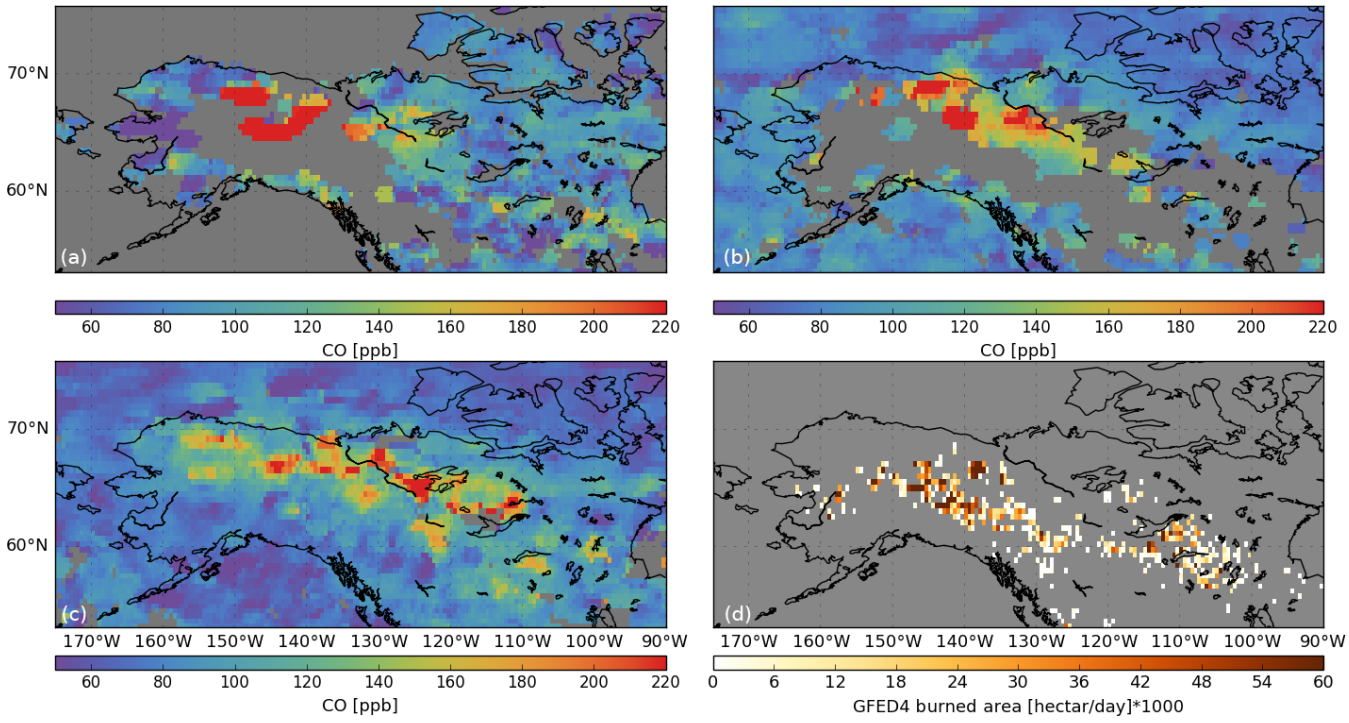

Figure 5. Same as Fig. 3 but for Alaska–Canada. The data are averaged from 1 July to 1 August 2004.

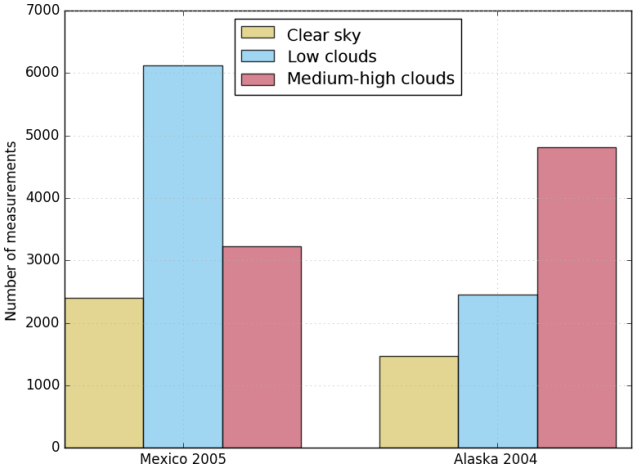

Figure 6. Number of individual SCIAMACHY CO retrievals under clear-sky (yellow), low-cloud (blue) and medium–high-cloud (pink) atmospheric conditions for the time range and latitude–longitude box specified in Figs. 3 and 5.

cloud and medium–high-cloud retrievals. Then we applied the oversampling approach with a longitude–latitude grid of $\delta = 0.05°$ (≤ 5.5 km) and an averaging radius $r = 40$ km (Figs. 7, 8 and 9). Subsequently, we calculated the CO enhancement for the three cities with respect to the background signal by estimating the difference between the median CO concentration inside and outside the urban area contours (Schneider et al., 2009). Obviously, the separation of urban and background CO concentrations cannot fully succeed due to the SCIAMACHY pixel size, the averaging approach and atmospheric transport. However the values presented in Fig. 11 give a first indication of enhanced CO due to the urban population.

For all three cities, we find that the CO enhancements of clear-sky observations coincide with the MODIS urban area contours. Furthermore, in the case of Paris we detect enhanced CO levels near the neighbouring city Rouen caused by local emissions or transport from the remote pollution of Paris (see Fig. 7). The strongest CO enhancement under the clear-sky condition occurs for Tehran with 8.1 ppb, closely followed by Los Angeles with 6.3, and the weakest enhancement we observe for Paris is 4.3 ppb. This difference can be explained by the different source strengths but is also influenced by the measurement statistics. The detection of urban CO concentration under low-cloud conditions perform comparably well with an enhancement of 8.8 ppb for Tehran, 8.3 ppb for Los Angeles and 3.4 ppb for Paris, where for Tehran and Los Angeles the spatial distribution of the enhancements agrees even better with the urban area contours. For observations with medium–high clouds, we see a less distinct CO enhancement over the three cities with 7.0 ppb for Tehran, 3.6 ppb for Los Angeles and only 1.8 ppb for Paris. Medium–high clouds shield the atmosphere below and so the retrieval is less sensitive to the city pollution estimates of the CO column from the measurement sensitivity above the cloud as already indicated by the column averaging ker-

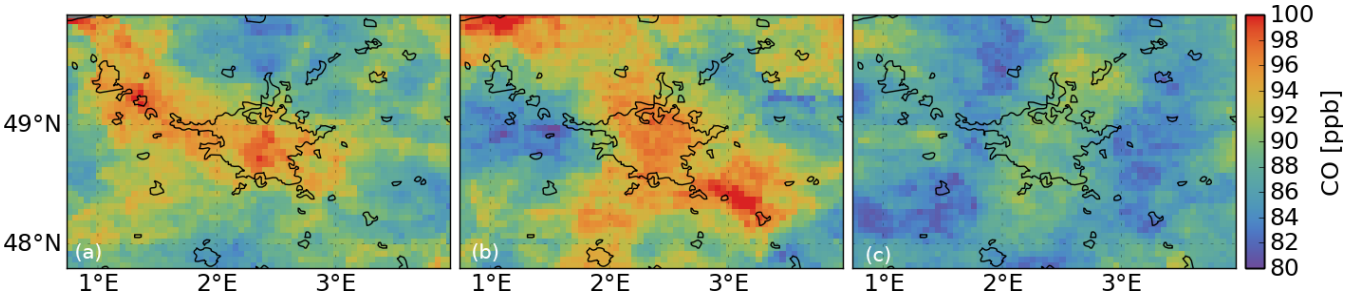

Figure 7. SCIAMACHY CO column mixing ratio averaged from January 2003 to April 2012 under clear-sky **(a)**, low-cloud **(b)** and medium–high-cloud **(c)** atmospheric conditions above Paris. The spatial sampling of the plot is $\delta = 0.05°$ in latitude and longitude and the data are averaged with radius $r = 40$ km. The urban area contours are based on MODIS measurements (Schneider et al., 2009).

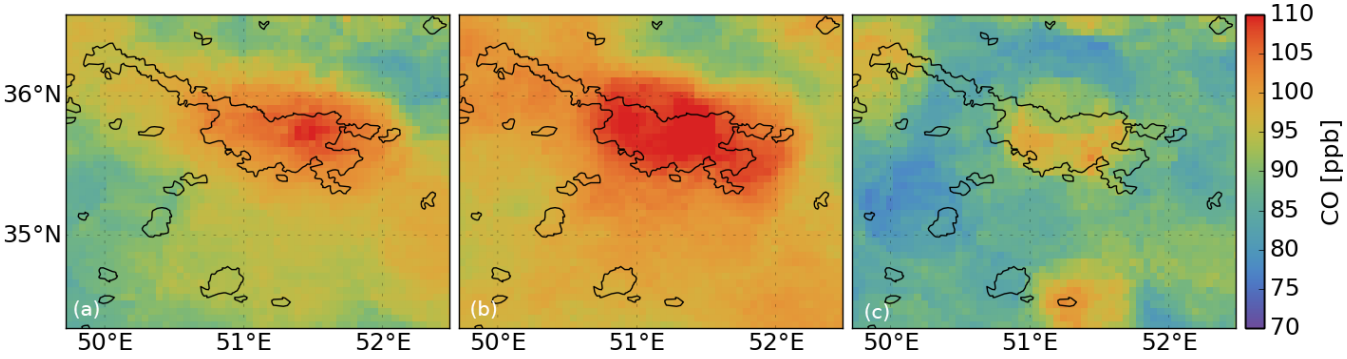

Figure 8. Same as Fig. 7 but for Tehran.

nels in Fig. 1. Consequently, measurements contaminated by medium–high clouds in combination with clear-sky and low-cloud retrievals can reveal information about the strength and vertical extension of the CO pollution.

Furthermore, including the cloudy retrievals improves the measurement statistics as indicated in Fig. 10. Including cloud-contaminated soundings means about double the amount of data is available for Tehran (a factor of 2.1), Paris (a factor of 2.6) and Los Angeles (a factor of 1.8). The relative amount of cloud-contaminated measurements differs significantly per city and is summarised in Table 2. Tehran and Los Angeles show similar distributions with a high number of clear-sky and low-cloud observations, whereas for Paris cloudy measurements are more predominant. Overall, we conclude that for the SCIAMACHY mission, cloud-contaminated measurements provide valuable and complementary information to clear-sky measurements.

Table 2. Number of clear-sky and cloud-contaminated measurements for the cities Tehran, Paris and Los Angeles. The absolute number of observations are given in brackets.

Cities	Clear-sky	Low cloud	Medium–high cloud
Tehran	47 % (2674)	44 % (2501)	9 % (537)
Los Angeles	55 % (2557)	35 % (1630)	10 % (482)
Paris	38 % (1338)	22 % (766)	40 % (1388)

5 Implications for TROPOMI

The TROPOMI instrument was successfully launched on the ESA's Sentinel-5 Precursor mission on 13 October 2017. The 2.3 µm spectral range is covered both by TROPOMI and SCIAMACHY with the same spectral resolution, whereby TROPOMI shows an improved radiometric performance with a high spatial resolution of up to 7×7 km^2 and with daily global coverage. The spectral analogy of TROPOMI and SCIAMACHY allowed us to apply the operational TROPOMI CO retrieval algorithm SICOR to the SCIAMACHY spectra to test its performance for cloud-contaminated measurements in preparation of TROPOMI data exploitation.

The spatial sampling of continuous TROPOMI nadir SWIR measurements with a swath of 2600 km provides 300 times more soundings compared to the limb-nadir observations of SCIAMACHY with a ground pixel size of 120×30 km and a swath of 960 km. Due to the higher SNR of TROPOMI SWIR measurements, CO total column will be provided with a precision < 10 % (Landgraf et al., 2016a, b) compared to the SCIAMACHY CO column precisions of 100 % and above (Gloudemans et al., 2008). Also, the radiometric accuracy is significantly improved, leading to a over-

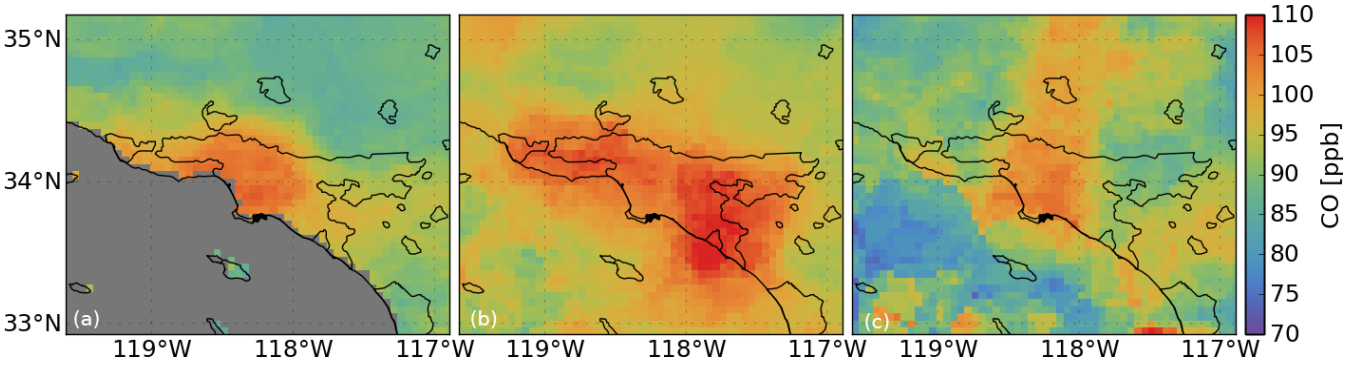

Figure 9. Same as Fig. 7 but for Los Angeles.

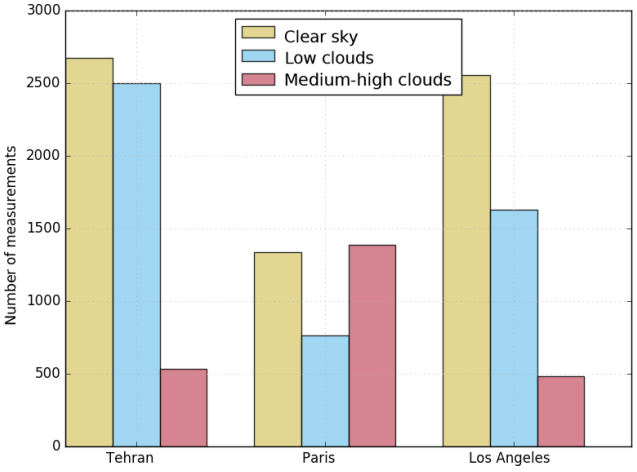

Figure 10. Number of individual SCIAMACHY CO retrievals under clear-sky (yellow), low-cloud (blue) and medium–high-cloud (pink) atmospheric condition for the time range and latitude–longitude box specified in Figs. 7, 8 and 9.

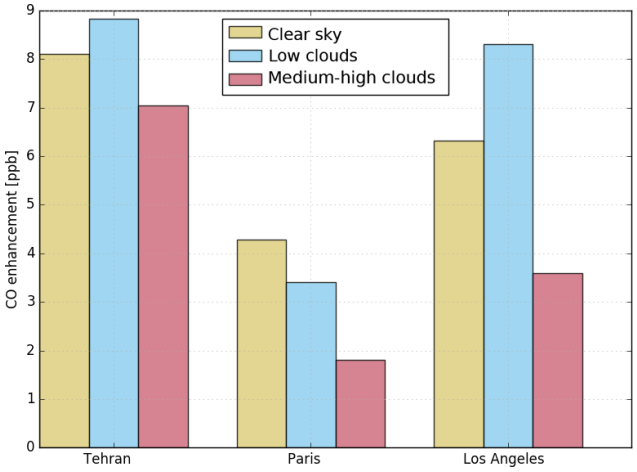

Figure 11. CO enhancement over cities shown in Figs. 7, 8 and 9 relative to the background concentration under clear-sky (yellow), low-cloud (blue) and medium–high-cloud (pink) atmospheric conditions. The difference between the median CO concentration inside and outside the urban area contours of each city is shown.

all bias estimate of the TROPOMI CO columns $< 10\,\%$ for clear-sky and cloudy observations (Landgraf et al., 2016a, b). Therefore, TROPOMI SWIR measurements will capture burning events, with atmospheric CO signatures significantly weaker than investigated in this study and urban pollution on a day-to-day basis with high spatial resolution and without precedent. Here, using cloudy data complementary to clear-sky observations will give us a new opportunity to study the vertical and horizontal distributions of atmospheric CO pollution. The first results of the TROPOMI CO data set are reported in Borsdorff et al. (2018).

6 Summary and conclusions

In this study, we discussed the benefit of using CO total column retrievals from cloud-contaminated SCIAMACHY 2.3 µm SWIR spectra to study pollution from cities and wildfires complementary to clear-sky soundings. For this purpose, we applied the SICOR algorithm to SCIAMACHY observations. SICOR was developed for the operational processing of the SWIR measurements of the TROPOMI instrument on ESA's Sentinel-5 Precursor. SICOR provides a possibility to retrieve effective cloud parameters together with trace gas columns. To investigate its capability to detect localized CO enhancements at urban areas and wildfires, we distinguished between retrievals under clear-sky, low-cloud and medium–high-cloud atmospheric conditions. As an example, we analysed CO enhancements over the cities Paris, Los Angeles and Tehran as well as the wildfire events in Mexico–Guatemala 2005 and Alaska–Canada 2004.

After data averaging over the entire mission period, we found that SCIAMACHY mean clear-sky observations can detect weak CO enhancements of less than 10 ppb over the three considered cities and coincide with the MODIS urban area contours. For Paris, we detected enhanced CO values next to the neighbouring city of Rouen, which can be

caused by the city itself or transport of remote pollution from Paris. Furthermore, clear-sky retrievals turned out to be suitable for locating the source of biomass burning in Mexico–Guatemala in agreement with most of the burned area reported by the daily GFED4 product. Here, the sensitivity of SWIR measurements to CO throughout the atmosphere including the planetary boundary layer makes clear-sky retrievals a preferable choice for the detection of such sources. However, only a fraction of all measurements fall into this category. For example, due to the meteorological situation during the Alaska–Canada 2004 burning event, insufficient clear-sky measurements were available to fully capture the wildfires. Moreover, the noise of the retrievals strongly depends on the surface reflectivity. We found clear-sky retrievals for the wildfires in Mexico–Guatemala 2005 inferior to cloudy retrievals regarding the noise performance (clouds are highly reflective in the SWIR) and the temporal and spatial sampling.

Considering pollution from cities, the CO retrieval works equally well for clear-sky and low-cloud measurements. This is probably because both are sensitive to CO in the planetary boundary layer. Compared to clear-sky observations, the temporal and spatial sampling of low-cloud observations improves the spatial match of the CO enhancements with the corresponding MODIS urban areas of Tehran and Los Angeles. The low-cloud retrievals of the 2005 wildfires in Mexico–Guatemala provide complementary information compared to clear-sky retrievals, indicating the CO outflow over the Gulf of Mexico and the Pacific Ocean, which is confirmed by smoke observations of the MODIS/Aqua instrument. Here, the high reflectivity of the clouds allows for the retrieval of CO over oceans, which was not possible with clear-sky measurements due to the dark ocean surface in the SWIR spectral range.

However, when using medium–high clouds for the detection of CO pollution we recognized a significant reduction in the CO enhancement above the three cities. Here, clouds shield the CO pollution and, consequently, the retrieval underestimates the total column of CO. This effect differs for the three cities. While the pollution from Tehran and Los Angeles is still present in the data product for medium–high clouds, it nearly vanishes for Paris, pointing to a CO enhancement localized in the lowest altitude range. Comparing low- and medium–high-cloud conditions for the Mexico fires, the CO enhancement is detected equally well, which indicates that the CO emission by this strong burning reaches the free troposphere. These examples show that CO retrievals for different cloud conditions are valuable for gaining information about the vertical extent of the atmospheric CO pollution.

Overall, the study of SCIAMACHY CO retrievals from cloud-contaminated 2.3 µm measurements showed the additive value of the data product compared to clear-sky retrievals when studying CO pollution on regional and urban scales. Particularly in perspective of the upcoming Sentinel-5 Precursor mission with the TROPOMI instrument as its single payload, the corresponding CO data product will open up new research opportunities due to the groundbreaking capabilities of the TROPOMI instrument.

Data availability. The full-mission SCIAMACHY CO data set used in this study, including clear-sky and cloudy-sky observations, is available for download at ftp://ftp.sron.nl/pub/pub/DataProducts/SCIAMACHY_CO/ (last access: 30 April 2018). The underlying data of the figures presented in this publication can be found at ftp://ftp.sron.nl/open-access-data/ (last access: 30 April 2018).

Competing interests. The authors declare that they have no conflict of interest.

Acknowledgements. SCIAMACHY is a joint project by the German Space Agency DLR and the Dutch Space Agency NSO with a contribution from the Belgian Space Agency. This research has been funded in part by the TROPOMI national programme from the Netherlands Space Office (NSO). Simulations were carried out on the Dutch national e-infrastructure with the support of SURF Cooperative.

Edited by: Frank Hase
Reviewed by: two anonymous referees

References

Borsdorff, T., Hasekamp, O. P., Wassmann, A., and Landgraf, J.: Insights into Tikhonov regularization: application to trace gas column retrieval and the efficient calculation of total column averaging kernels, Atmos. Meas. Tech., 7, 523–535, https://doi.org/10.5194/amt-7-523-2014, 2014.

Borsdorff, T., Tol, P., Williams, J. E., de Laat, J., aan de Brugh, J., Nédélec, P., Aben, I., and Landgraf, J.: Carbon monoxide total columns from SCIAMACHY 2.3 µm atmospheric reflectance measurements: towards a full-mission data product (2003–2012), Atmos. Meas. Tech., 9, 227–248, https://doi.org/10.5194/amt-9-227-2016, 2016.

Borsdorff, T., aan de Brugh, J., Hu, H., Nédélec, P., Aben, I., and Landgraf, J.: Carbon monoxide column retrieval for clear-sky and cloudy atmospheres: a full-mission data set from SCIAMACHY 2.3 µm reflectance measurements, Atmos. Meas. Tech., 10, 1769–1782, https://doi.org/10.5194/amt-10-1769-2017, 2017.

Borsdorff, T., de Brugh, J. A., Hu, H., Aben, I., Hasekamp, O., and Landgraf, J.: Measuring Carbon Monoxide With TROPOMI: First Results and a Comparison With ECMWF-IFS Analysis Data, Geophys. Res. Lett., 45, 2826–2832, https://doi.org/10.1002/2018GL077045, 2018.

Bovensmann, H., Burrows, J. P., Buchwitz, M., Frerick, J., Noël, S., Rozanov, V. V., Chance, K. V., and Goede, A. P. H.: SCIAMACHY: Mission Objectives and Measurement Modes,

J. Atmos. Sci., 56, 127–150, https://doi.org/10.1175/1520-0469(1999)056<0127:smoamm>2.0.co;2, 1999.

Buchwitz, M., de Beek, R., Bramstedt, K., Noël, S., Bovensmann, H., and Burrows, J. P.: Global carbon monoxide as retrieved from SCIAMACHY by WFM-DOAS, Atmos. Chem. Phys., 4, 1945–1960, https://doi.org/10.5194/acp-4-1945-2004, 2004.

Buchwitz, M., Khlystova, I., Bovensmann, H., and Burrows, J. P.: Three years of global carbon monoxide from SCIAMACHY: comparison with MOPITT and first results related to the detection of enhanced CO over cities, Atmos. Chem. Phys., 7, 2399–2411, https://doi.org/10.5194/acp-7-2399-2007, 2007.

Clerbaux, C., Edwards, D. P., Deeter, M., Emmons, L., Lamarque, J.-F., Tie, X. X., Massie, S. T., and Gille, J.: Carbon monoxide pollution from cities and urban areas observed by the Terra/MOPITT mission, Geophys. Res. Lett., 35, l03817, https://doi.org/10.1029/2007GL032300, 2008.

Deeter, M. N.: Operational carbon monoxide retrieval algorithm and selected results for the MOPITT instrument, J. Geophys. Res., 108, 4399, https://doi.org/10.1029/2002jd003186, 2003.

de Laat, A. T. J., Gloudemans, A. M. S., Schrijver, H., van den Broek, M. M. P., Meirink, J. F., Aben, I., and Krol, M.: Quantitative analysis of SCIAMACHY carbon monoxide total column measurements, Geophys. Res. Lett., 33, l07807, https://doi.org/10.1029/2005GL025530, 2006.

de Laat, A. T. J., Gloudemans, A. M. S., Aben, I., Krol, M., Meirink, J. F., van der Werf, G. R., and Schrijver, H.: Scanning Imaging Absorption Spectrometer for Atmospheric Chartography carbon monoxide total columns: Statistical evaluation and comparison with chemistry transport model results, J. Geophys. Res., 112, D12310, https://doi.org/10.1029/2006jd008256, 2007.

de Laat, A. T. J., Dijkstra, R., Schrijver, H., Nédélec, P., and Aben, I.: Validation of six years of SCIAMACHY carbon monoxide observations using MOZAIC CO profile measurements, Atmos. Meas. Tech., 5, 2133–2142, https://doi.org/10.5194/amt-5-2133-2012, 2012.

Fioletov, V. E., McLinden, C. A., Krotkov, N., Moran, M. D., and Yang, K.: Estimation of SO2 emissions using OMI retrievals, Geophys. Res. Lett., 38, l21811, https://doi.org/10.1029/2011GL049402, 2011.

Frankenberg, C., Platt, U., and Wagner, T.: Retrieval of CO from SCIAMACHY onboard ENVISAT: detection of strongly polluted areas and seasonal patterns in global CO abundances, Atmos. Chem. Phys., 5, 1639–1644, https://doi.org/10.5194/acp-5-1639-2005, 2005.

Gimeno García, S., Schreier, F., Lichtenberg, G., and Slijkhuis, S.: Near infrared nadir retrieval of vertical column densities: methodology and application to SCIAMACHY, Atmos. Meas. Tech., 4, 2633–2657, https://doi.org/10.5194/amt-4-2633-2011, 2011.

Gloudemans, A. M. S., Krol, M. C., Meirink, J. F., de Laat, A. T. J., van der Werf, G. R., Schrijver, H., van den Broek, M. M. P., and Aben, I.: Evidence for long-range transport of carbon monoxide in the Southern Hemisphere from SCIAMACHY observations, Geophys. Res. Lett., 33, L16807, https://doi.org/10.1029/2006gl026804, 2006.

Gloudemans, A. M. S., Schrijver, H., Hasekamp, O. P., and Aben, I.: Error analysis for CO and CH_4 total column retrievals from SCIAMACHY 2.3 µm spectra, Atmos. Chem. Phys., 8, 3999–4017, https://doi.org/10.5194/acp-8-3999-2008, 2008.

Gloudemans, A. M. S., de Laat, A. T. J., Schrijver, H., Aben, I., Meirink, J. F., and van der Werf, G. R.: SCIAMACHY CO over land and oceans: 2003–2007 interannual variability, Atmos. Chem. Phys., 9, 3799–3813, https://doi.org/10.5194/acp-9-3799-2009, 2009.

Herrera, G. V.: Mexican forest fires and their decadal variations, Adv. Space Res., 58, 2104–2115, https://doi.org/10.1016/j.asr.2016.08.030, 2016.

Holloway, T., Levy, H., and Kasibhatla, P.: Global distribution of carbon monoxide, J. Geophys. Res.-Atmos., 105, 12123–12147, https://doi.org/10.1029/1999jd901173, 2000.

Krijger, J. M., Aben, I., and Schrijver, H.: Distinction between clouds and ice/snow covered surfaces in the identification of cloud-free observations using SCIAMACHY PMDs, Atmos. Chem. Phys., 5, 2729–2738, https://doi.org/10.5194/acp-5-2729-2005, 2005.

Krijger, J. M., Tol, P., Istomina, L. G., Schlundt, C., Schrijver, H., and Aben, I.: Improved identification of clouds and ice/snow covered surfaces in SCIAMACHY observations, Atmos. Meas. Tech., 4, 2213–2224, https://doi.org/10.5194/amt-4-2213-2011, 2011.

Landgraf, J., aan de Brugh, J., Borsdorff, T., Houweling, S., and Hasekamp, O.: Algorithm Theoretical Baseline Document for Sentinel-5 Precursor: Carbon Monoxide Total Column Retrieval, Atbd, SRON, Sorbonnelaan 2, 3584 CA Utrecht, the Netherlands, 2016a.

Landgraf, J., aan de Brugh, J., Scheepmaker, R., Borsdorff, T., Hu, H., Houweling, S., Butz, A., Aben, I., and Hasekamp, O.: Carbon monoxide total column retrievals from TROPOMI shortwave infrared measurements, Atmos. Meas. Tech., 9, 4955–4975, https://doi.org/10.5194/amt-9-4955-2016, 2016b.

Liu, C., Beirle, S., Butler, T., Hoor, P., Frankenberg, C., Jöckel, P., Penning de Vries, M., Platt, U., Pozzer, A., Lawrence, M. G., Lelieveld, J., Tost, H., and Wagner, T.: Profile information on CO from SCIAMACHY observations using cloud slicing and comparison with model simulations, Atmos. Chem. Phys., 14, 1717–1732, https://doi.org/10.5194/acp-14-1717-2014, 2014.

Logan, J. A., Prather, M. J., Wofsy, S. C., and McElroy, M. B.: Tropospheric chemistry: A global perspective, J. Geophys. Res., 86, 7210, https://doi.org/10.1029/jc086ic08p07210, 1981.

McMillan, W. W.: Daily global maps of carbon monoxide from NASA's Atmospheric Infrared Sounder, Geophys. Res. Lett., 32, L11801, https://doi.org/10.1029/2004gl021821, 2005.

Pfister, G., Hess, P. G., Emmons, L. K., Lamarque, J.-F., Wiedinmyer, C., Edwards, D. P., PÈtron, G., Gille, J. C., and Sachse, G. W.: Quantifying CO emissions from the 2004 Alaskan wildfires using MOPITT CO data, Geophys. Res. Lett., 32, l11809, https://doi.org/10.1029/2005GL022995, 2005.

Pommier, M., McLinden, C. A., and Deeter, M.: Relative changes in CO emissions over megacities based on observations from space, Geophys. Res. Lett., 40, 3766–3771, https://doi.org/10.1002/grl.50704, 2013.

Randerson, J., van der Werf, G., Giglio, L., Collatz, G., and Kasibhatla, P.: Global Fire Emissions Database, Version 4.1 (GFEDv4), https://doi.org/10.3334/ornldaac/1293, 2017.

Rinsland, C. P., Luo, M., Logan, J. A., Beer, R., Worden, H., Kulawik, S. S., Rider, D., Osterman, G., Gunson, M., Eldering, A., Goldman, A., Shephard, M., Clough, S. A., Rodgers, C., Lampel, M., and Chiou, L.: Nadir measurements of carbon monox-

ide distributions by the Tropospheric Emission Spectrometer instrument onboard the Aura Spacecraft: Overview of analysis approach and examples of initial results, Geophys. Res. Lett., 33, L22806, https://doi.org/10.1029/2006gl027000, 2006.

Rodgers, C. D.: Inverse methods for atmospheric sounding : theory and practice, Series on atmospheric, oceanic and planetary physics, vol. 2, World Scientific, Singapore, River Edge, N.J., reprint: 2004, 2008, 2000.

Schneider, A., Friedl, M. A., and Potere, D.: A new map of global urban extent from MODIS satellite data, Environ. Res. Lett., 4, 044003, 044003, 2009.

Spivakovsky, C. M., Logan, J. A., Montzka, S. A., Balkanski, Y. J., Foreman-Fowler, M., Jones, D. B. A., Horowitz, L. W., Fusco, A. C., Brenninkmeijer, C. A. M., Prather, M. J., Wofsy, S. C., and McElroy, M. B.: Three-dimensional climatological distribution of tropospheric OH: Update and evaluation, J. Geophys. Res.-Atmos., 105, 8931–8980, https://doi.org/10.1029/1999jd901006, 2000.

Turquety, S., Hadji-Lazaro, J., Clerbaux, C., Hauglustaine, D. A., Clough, S. A., Cassé, V., Schlüssel, P., and Mégie, G.: Operational trace gas retrieval algorithm for the Infrared Atmospheric Sounding Interferometer, J. Geophys. Res.-Atmos., 109, D21301, https://doi.org/10.1029/2004jd004821, 2004.

Veefkind, J., Aben, I., McMullan, K., Förster, H., de Vries, J., Otter, G., Claas, J., Eskes, H., de Haan, J., Kleipool, Q., van Weele, M., Hasekamp, O., Hoogeveen, R., Landgraf, J., Snel, R., Tol, P., Ingmann, P., Voors, R., Kruizinga, B., Vink, R., Visser, H., and Levelt, P.: TROPOMI on the ESA Sentinel-5 Precursor: A GMES mission for global observations of the atmospheric composition for climate, air quality and ozone layer applications, Remote Sens. Environ., 120, 70–83, https://doi.org/10.1016/j.rse.2011.09.027, 2012.

Vidot, J., Landgraf, J., Hasekamp, O., Butz, A., Galli, A., Tol, P., and Aben, I.: Carbon monoxide from shortwave infrared reflectance measurements: A new retrieval approach for clear sky and partially cloudy atmospheres, Remote Sens. Environ., 120, 255–266, https://doi.org/10.1016/j.rse.2011.09.032, 2012.

Williams, J. E., van Velthoven, P. F. J., and Brenninkmeijer, C. A. M.: Quantifying the uncertainty in simulating global tropospheric composition due to the variability in global emission estimates of Biogenic Volatile Organic Compounds, Atmos. Chem. Phys., 13, 2857–2891, https://doi.org/10.5194/acp-13-2857-2013, 2013.

Williams, J. E., Le Bras, G., Kukui, A., Ziereis, H., and Brenninkmeijer, C. A. M.: The impact of the chemical production of methyl nitrate from the $NO + CH_3O_2$ reaction on the global distributions of alkyl nitrates, nitrogen oxides and tropospheric ozone: a global modelling study, Atmos. Chem. Phys., 14, 2363–2382, https://doi.org/10.5194/acp-14-2363-2014, 2014.

Yurganov, L. N., Duchatelet, P., Dzhola, A. V., Edwards, D. P., Hase, F., Kramer, I., Mahieu, E., Mellqvist, J., Notholt, J., Novelli, P. C., Rockmann, A., Scheel, H. E., Schneider, M., Schulz, A., Strandberg, A., Sussmann, R., Tanimoto, H., Velazco, V., Drummond, J. R., and Gille, J. C.: Increased Northern Hemispheric carbon monoxide burden in the troposphere in 2002 and 2003 detected from the ground and from space, Atmos. Chem. Phys., 5, 563–573, https://doi.org/10.5194/acp-5-563-2005, 2005.